SUPPLEMENTARY METHODS

DNA sequence design

The high-level structures of the strands and complexes were designed based on biophysical expectations of the stability of the complexes and their dynamic interactions with the other components of the system. The conserved sequences of the catalytic cores of the 8-17 and E6 DNAzymes were obtained from the literature [1, 2].

Sequence design for SCS molecules was performed using a custom Python script that uses the NUPACK secondary structure prediction algorithm [3] and the ISO numeric representation of nucleic acid secondary structure [4] to find suitable domain assignments for the SCS sequence. Randomly generated sequences were tested using NUPACK to assess their equilibrium binding to the downstream DNAzyme and inhibitor strands in both the pre-cleavage state (to estimate leak rates) and the post-cleavage state (to estimate activation rates). Sequences that passed these tests were assessed for unwanted secondary structure using NUPACK and ISO, and candidate sequences were manually checked and optimized. Sequences for loop-inhibited DNAzyme logic gates were derived from the sequences of the DNAzyme displacement logic gates in the two-layer cascade via ensemble defect optimization using the NUPACK design tool [5].

For the dengue serotyping bioassays, we first performed a ClustalW sequence alignment on the genomes of all four dengue serotypes. Conserved and unconserved regions were identified manually and candidate target sequences were selected from these regions. These were then tested for secondary structure using NUPACK and optimized by hand as necessary.

It is worth noting that NUPACK only models systems at thermodynamic equilibrium, and because the SCS participates in highly dynamic, transient interactions we can only draw limited conclusions about the behavior of our circuits from NUPACK predictions. We were forced to approximate the ribose base at the cleavage site by a deoxyribose base, because the available thermodynamic tables that serve as the basis of the NUPACK structure prediction algorithm [6] do not include parameters for DNA-RNA hybrids. Furthermore, the thermodynamic tables are only strictly valid within a certain range of salt concentrations. In particular, our reactions require Zn^{2+} ions in the buffer to serve as cofactors for the DNAzyme cleavage reaction, and the effects of these ions on DNA folding and on the relative stability of the various DNA structures are subjects of ongoing research [7-11].

Oligonucleotide sequences

Oligonucleotide sequences are presented in Tables S1-8. All sequences are listed 5' to 3'. Substrates are cleaved at the dinucleotide junction between the tow bases highlighted in red, and the catalytic cores of DNAzymes are highlighted in boldface. The RNA base at the cleavage site in each substrate (including SCS) strand is represented as rA. Fluorescein fluorophores and TAMRA quenchers are represented as /FAM/ and /TAM/ respectively.

Multi-layer cascade experiments (Figure 2b,c)

Sequences are listed in Table S1. Concentrations for Figure 2b: 100 nM DNAzyme per layer, 125 nM inhibitor per layer (except the top layer), 100 nM SCS per layer, 250 nM

fluorescent reporter substrate. Concentrations for Figure 2c: 100 nM layer 1 DNAzyme, 75 nM layer 2 DNAzyme, 50 nM layer 3 DNAzyme, 25 nM layer 4 DNAzyme, 25% excess inhibitor and equimolar SCS per layer relative to DNAzyme concentration, 250 nM fluorescent reporter substrate.

Pre-annealed DNAzyme-inhibitor complexes were added to buffer first, then pre-annealed SCS molecules, then fluorescent reporter substrate. Input (active DNAzyme in the top layer) was added last to initiate the reaction. Loss of FRET was observed over two hours. Each trace was baseline-corrected by subtracting the initial value for that trace from each time point in that trace, ensuring that each trace was plotting starting from zero fluorescence.

Characterization of two-layer dengue serotyping circuits (Figure 3b, Figure S4) and secondary structure optimization in dengue serotyping circuits (Figure S5b,d)

Sequences for Figure 3b and Figure S4 are listed in Table S2. Sequences for Figure S5b are listed in Table S7. Sequences for Figure S5d are listed in Table S8. Concentrations: 100 nM DNAzyme (upstream & downstream), 125 nM inhibitor (upstream & downstream), 100 nM inputs (DengueA, DengueB, DEN-k for k=1,2,3,4 as appropriate), 250 nM fluorescent reporter substrate. In Figure S4, experiments using multiple serotype-specific input strands were run using 100 nM of *each* serotype-specific input.

Pre-annealed DNAzyme-inhibitor complexes were added to buffer first, then pre-annealed SCS molecules, then inputs. The system was incubated at room temperature for 2 hours, then fluorescent reporter substrate was added, and the endpoint fluorescence value was observed after incubation at room temperature for a further 6 hours (2 hours for Figure S5b,d). All endpoint fluorescence values were baseline-corrected relative to the corresponding fluorescence value at the time of substrate addition. In Figure 3b and Figure S4, the baseline-corrected fluorescence values were normalized to the endpoint fluorescence of the positive trace, so that values between 0 and 1 could be reported. In Figure S5b,d, the baseline-corrected fluorescence values were plotted with no further data processing.

Concentration profile of two-layer DNAzyme signaling cascade (Figure S1)

Sequences are listed in Table S1. Concentrations: DNAzyme concentrations (upstream & downstream) and SCS molecules and inputs varied according to the figure legend. In each case, downstream inhibitor was used in 25% excess relative to the concentration of the downstream DNAzyme. 250 nM fluorescent reporter substrate was used.

Pre-annealed DNAzyme-inhibitor complexes were added to buffer first, then pre-annealed SCS molecules, then fluorescent reporter substrate. Inputs were added last to initiate the reaction. Loss of FRET was observed over 30 minutes. Raw fluorescence values were plotted with no additional data processing.

Demonstration that SCS cleavage is necessary for signal propagation (Figure S2)

Sequences are listed in Table S3. Concentrations: 100 nM DNAzymes (upstream & downstream), 125 nM inhibitor (downstream), 100 nM SCS (cleavable or uncleavable, as appropriate), 250 nM fluorescent reporter substrate.

Pre-annealed DNAzyme-inhibitor complexes were added to buffer first, then pre-annealed SCS molecules, then fluorescent reporter substrate. Active upstream DNAzyme was added last to initiate the reaction. Loss of FRET was observed over two hours. Raw fluorescence values were plotted with no additional data processing.

Demonstration of SCS input-output combinations (Figure S3a-c)

Sequences are listed in Tables S4-6. Concentrations: (a) 100 nM DNAzymes (upstream & downstream), 125 nM inhibitor (upstream & downstream), 100 nM SCS, 50 nM reporter substrate, 100 nM input 1, 100 nM input 2. (b) 100 nM DNAzymes (upstream & downstream), 125 nM inhibitor (upstream), 100 nM SCS, 50 nM reporter substrate, 100 nM input. (c) 100 nM DNAzyme (upstream), 125 DNAzyme inhibitor (upstream), 100 nM SCS, 100 nM input, 100 nM fluorescent reporter strand, 125 nM downstream inhibitor labeled with quencher.

Inhibited DNAzymes (either pre-annealed DNAzyme-inhibitor complexes or annealed loop-inhibited DNAzyme strands) were added to buffer first, then pre-annealed SCS molecules, then inputs. The system was incubated for 2 hours at room temperature, then the reporter (either a fluorescent reporter substrate or a strand displacement reporter complex) was added, and the endpoint fluorescence value was observed after a further 30 minutes incubation at room temperature. Each endpoint fluorescence value was baseline-corrected relative to the corresponding fluorescence value at substrate addition.

Two-layer cascade experiment in DNA background (Figure S6)

Sequences are listed in Table S1. Concentrations: 100 nM DNAzyme (layers 1 and 2), 125 nM inhibitor (layer 1), 100 nM SCS (SCS_2), 50 nM fluorescent reporter substrate (layer 1).

Herring sperm DNA (Promega, Madison, WI) was annealed (as described above) and various amounts were added to 96 well plates containing buffer. Pre-annealed downstream DNAzyme-inhibitor complexes were added first, then pre-annealed SCS molecules, then fluorescent reporter substrate. Input (active upstream DNAzyme) was added last to initiate the reaction. Loss of FRET was observed over 30 minutes. Each positive kinetic trace was baseline-corrected by subtracting each time point observed from a negative control (run in the same experimental conditions but no active upstream DNAzyme present) from the corresponding time point in each positive trace. None of the negative controls showed a significant increase in fluorescence.

SUPPLEMENTARY FIGURES

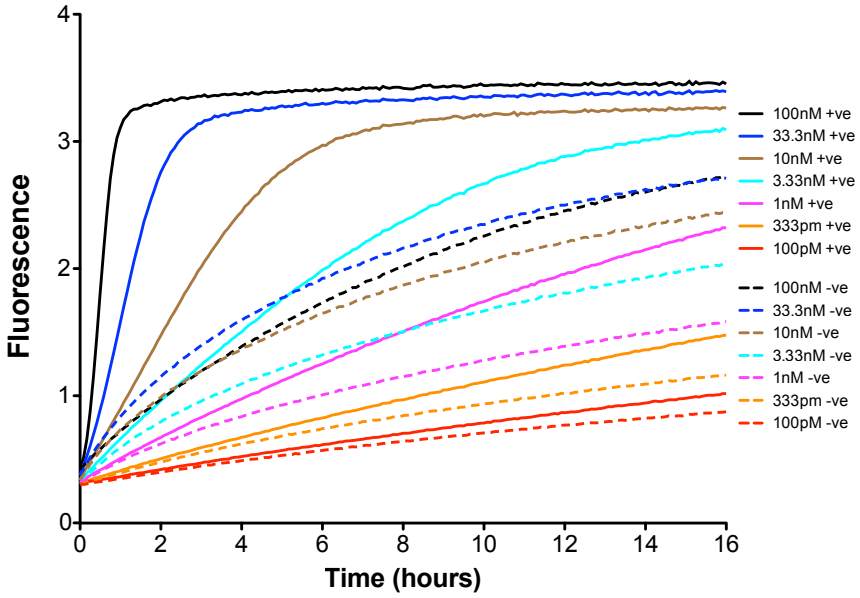

Figure S1: Concentration profile of two-layer DNAzyme signaling cascade. Broken lines indicate response in absence of active upstream DNAzymes (-ve control) and solid lines indicate response in presence of active upstream DNAzymes (+ve control). Concentrations of DNAzymes, inputs and SCS molecules vary as shown in the legend; inhibitor concentrations were also varied to ensure a 25% excess of inhibitor with respect to the DNAzyme concentration in each case. Concentration of the readout substrate was the same in all cases. Reducing the concentrations of circuit elements reduced both leakage rates and activation rates, as expected.

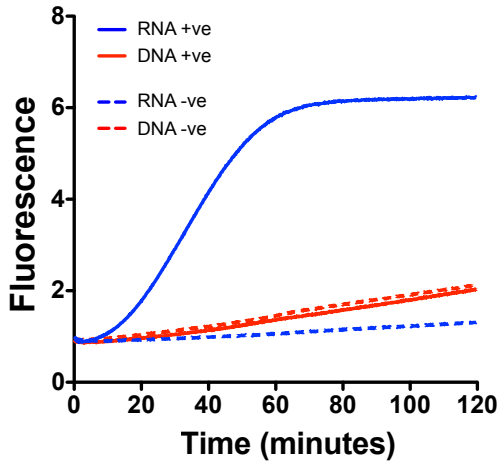

Figure S2: Demonstration that cleavage is required for signal propagation by the SCS in a two-layer cascade. Red traces are the response of an SCS molecule with the rA (ribose) base at the cleavage replaced by a dA (deoxyribose) base, both in the presence (+ve control, solid line) and absence (-ve control, broken line) of the upstream active DNAzyme. The substitution of dA for rA at the cleavage site makes the SCS molecule uncleavable. For comparison, the blue traces are the response of a cleavable SCS in the two layer cascade, both in the presence (solid line) and absence (broken line) of the upstream active DNAzyme. Addition of the upstream active DNAzyme does not produce any additional leakage in the case of the uncleavable SCS, which demonstrates that simply opening the outer stem by strand displacement does not produce downstream signal propagation. Hence, the cleavage step is required.

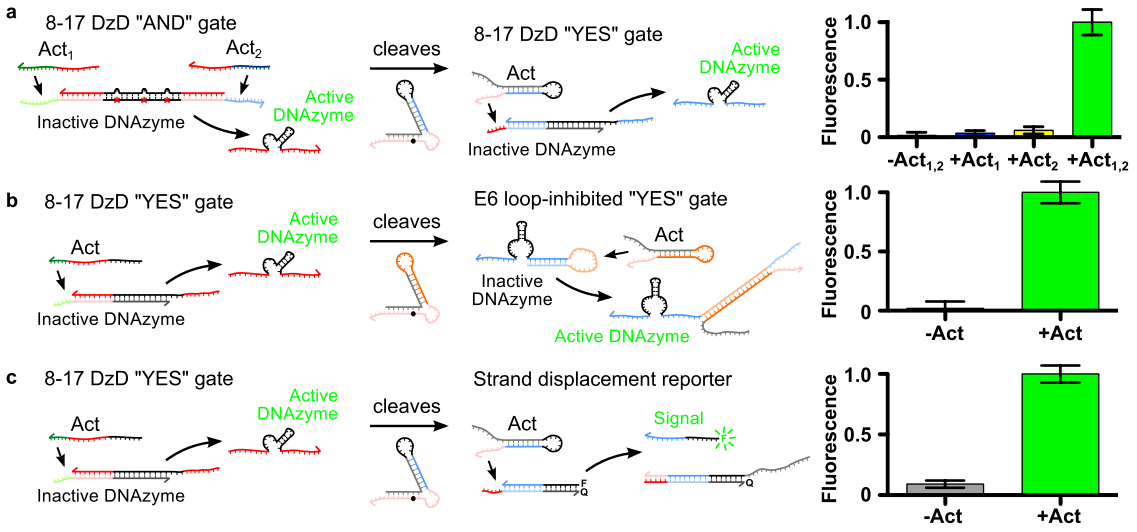

Figure S3. Application of the SCS as a generic interface molecule. An active DNAzyme from the input module cleaves the SCS, releasing an activator for the output module. This shows that our SCS design enables interoperability between different architectures, which is an important goal for future development of DNA logic circuits. Error bars on bar charts show the 95% confidence interval from triplicate runs of each experiment. a) Input module is a previously reported 8-17 DNAzyme displacement (DzD) “AND” gate with mismatched bases in the catalytic core portion of the inhibitor [12], which is activated by two inputs in a cooperative strand displacement reaction [13]. Output module is an 8-17 DzD “YES” gate. b) Input module is an 8-17 DzD “YES” gate, output module is a loop-inhibited “YES” gate based on the E6 catalytic motif [1]. Since the E6 DNAzyme cleaves the same dinucleotide junction as the 8-17 DNAzyme, we can use the same fluorescent reporter substrate in this case. c) Input module is an 8-17 DzD “YES” gate, output module is a DNA strand displacement reporter gate in which the activator released by cleavage of the SCS simply displaces a fluorescently-labeled strand from the reporter complex. The advantage of using a strand displacement gate as the reporter is that it does not amplify leakage, which might be preferable for certain applications. More generally, this reaction demonstrates that the SCS design could be used to interface DNAzymes with arbitrary strand displacement circuits and alternative DNAzyme catalytic motifs such as the 10-23 RNA-cleaving DNAzyme [2] and DNA-cleaving DNAzymes [14-16].

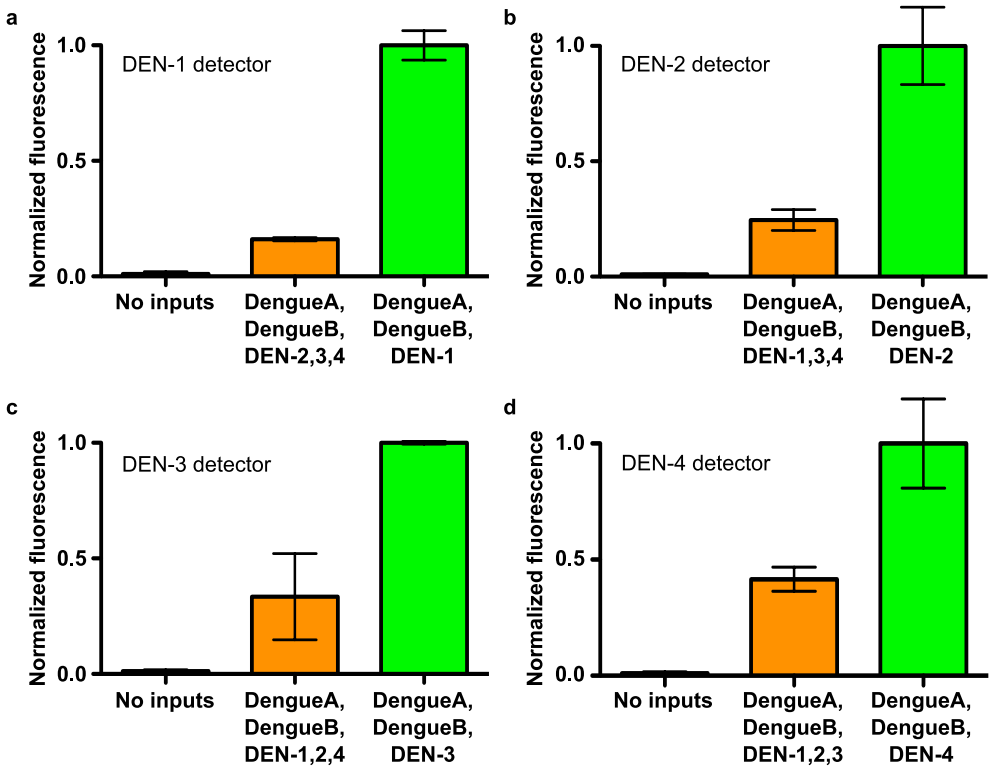

Figure S4: Demonstration of serotype-specific response from dengue serotyping circuits, which were presented in Figure 3. In each case, the negative control (grey) is the response in the absence of all three inputs, and the positive control (green) is the response in the presence of the two conserved inputs and the correct serotype-specific input (DEN-1, DEN-2, DEN-3 or DEN-4). The orange bar is the response in the presence of the two conserved inputs and all three incorrect serotype-specific sequences. **a**, Serotype specificity of DEN-1 detection circuit. **b**, Serotype specificity of DEN-2 detection circuit. **c**, Serotype specificity of DEN-3 detection circuit. **d**, Serotype specificity of DEN-4 detection circuit. In all cases, we observe a significantly reduced response when the incorrect serotype-specific sequences are present. In fact, the magnitudes of the non-specific responses to the incorrect serotype-sequences correlate with the background activations observed in the presence of the downstream DengueB input sequence in Figure 3, so it is likely that the non-specific activation seen in the presence of the incorrect serotype-specific sequences is in fact largely caused by the presence of DengueB. Hence we conclude that our four dengue detection circuits are in fact serotype-specific. Error bars represent the 95% confidence interval from three replicate experiments.

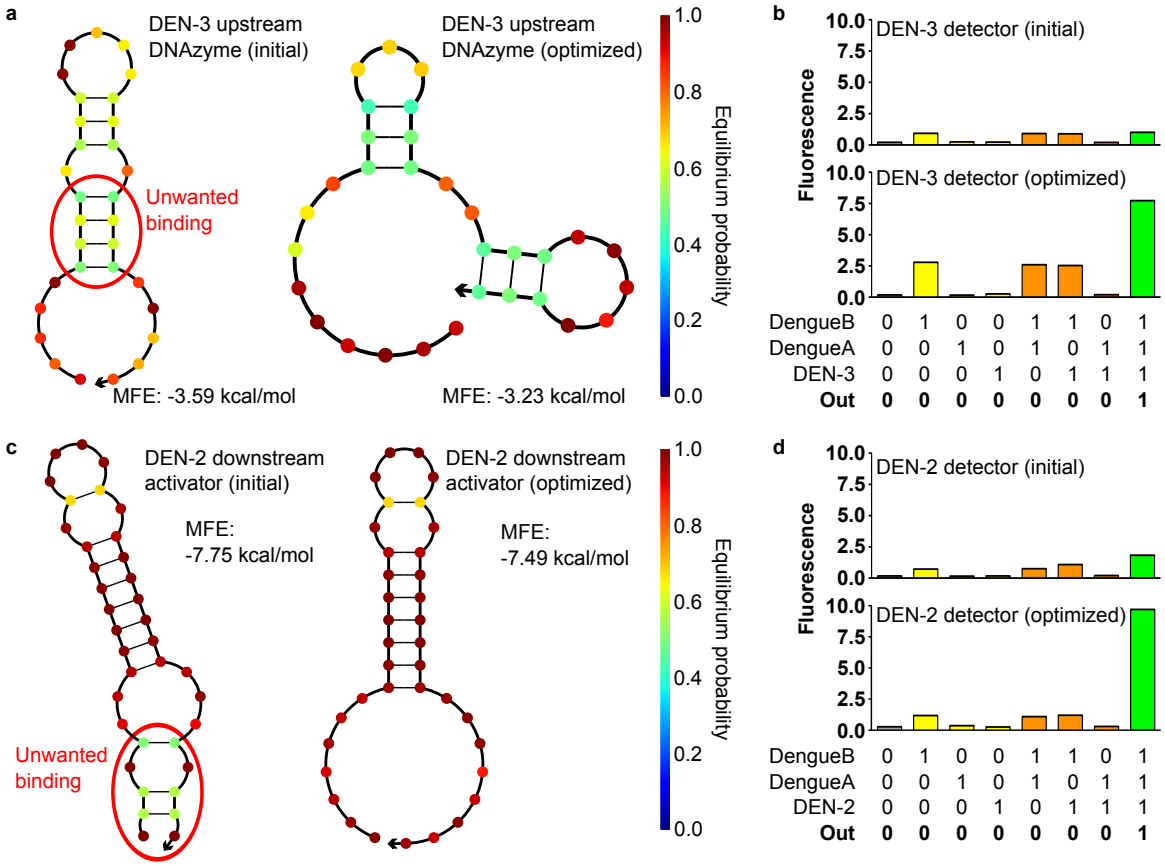

Figure S5: Performance improvements from secondary structure optimization of dengue serotyping circuit components. a, The upstream DNAzyme derived from the initial DEN-3 target sequence was found to have unwanted secondary structure, highlighted in red. We hypothesized that this would cause difficulty binding to the SCS molecule in the dengue serotyping circuit, because the two substrate binding arms of the DNAzyme were hybridized to each other. We switched to a different DEN-3 target sequence that removed this unwanted binding in the DNAzyme strand. **b**, Performance of the DEN-3 detection circuit using the initial and the optimized target sequences (and associated upstream DNAzymes and SCS molecules). The initial circuit produced no activation above background in the presence of all three inputs, whereas the optimized circuit produced a significant response in this case. **c**, The SCS cleavage product derived from the initial DEN-2 target sequence was found to have unwanted secondary structure, highlighted in red. We hypothesized that this would sequester the toehold of the downstream activator strand even after the SCS was cleaved, leading to low activation of the circuit. We switch to a different DEN-2 target sequence that removed this unwanted binding in the activator strand. **d**, Performance of the DEN-2 detection circuit using the initial and the optimized target sequences (and associated upstream DNAzymes and SCS molecules). The initial circuit produced little activation above background in the presence of all three inputs, whereas the optimized circuit produced a significant response in this case. This highlights the importance of design optimization to prevent the formation of unwanted structures. The bar charts are representative data that illustrate the performance difference between the initial and optimized versions of the circuits.

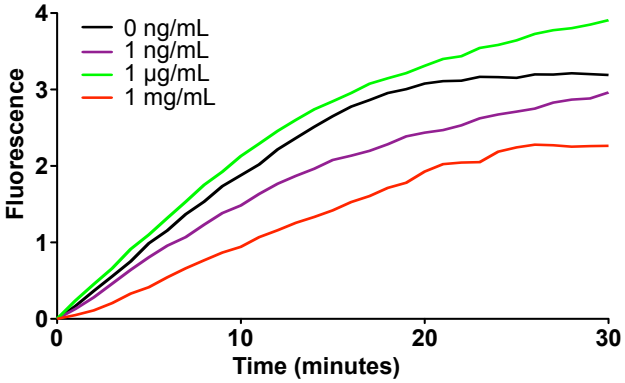

Figure S6. Operation of DNAzyme signaling cascades in the presence of background DNA. The two-layer cascade experiment was repeated in the presence of the labeled concentrations of denatured herring sperm DNA, covering six orders of magnitude from 1 ng/mL to 1 mg/mL. We observed no systematic loss of performance caused by the presence of background DNA. We hypothesize that the single-stranded SCS design allows rapid refolding following interactions with the background DNA, preventing spurious activation.

SUPPLEMENTARY TABLES

Table S1. Sequences from multi-layer cascade experiments (Figure 2b,c), concentration profile of two-layer DNAzyme signaling cascade (Figure S1), and two-layer cascade experiment in DNA background (Figure S6).

Strand	Sequence
Layer 5 DNAzyme	GGGAGCCGTCCGAGCCGGTCGAAACTGTGGT
SCS_5	GCCGCTATACAAAGGTCGAAATATTTGTACCACAGTrAGCGGCTCCC
Layer 4 DNAzyme	GGTAGCGC**TCCGAGCCGGTCGAA**ATATTTGT
Layer 4 inhibitor	GTGGTACAAATATTTCGACCGGC
SCS_4	GCGCCTATTCCCCGGTCGAAACAGGGGAACAAATATrAGGCGCTACC
Layer 3 DNAzyme	ACATGCCG**TCCGAGCCGGTCGAA**ACAGGGGA
Layer 3 inhibitor	TTTGTTCCCCTGTTTCGACCGGC
SCS_3	GCCGCTAATACATGGTCGAAAGTATGTATCCCCTGTrAGCGGCATGT
Layer 2 DNAzyme	ATCACGCC**TCCGAGCCGGTCGAA**AGTATGTA
Layer 2 inhibitor	GGGGATACATACTTTCGACCGGC
SCS_2	CGCCCTAATCTTAGGTCGAAAACTAAGATACATACTrAGGGCGTGATG
Layer 1 DNAzyme	GAACTATC**TCCGAGCCGGTCGAA**AACTAAGA
Layer 1 inhibitor	ATGTATCTTAGTTTTCGACCGGC
Layer 1 reporter substrate	/FAM/-TCTTAGTTrAGGATAGTTCAT-/TAM/

Table S2. Sequences from characterization of two-layer dengue serotyping circuits (Figure 3b and Figure S4).

Strand	Sequence
DEN-1 target	ACCAACAACAAACACCAAA
DEN-1 upstream DNAzyme	ACACCAAA**TCCGAGCCGGTCGAA**CATCATTC
DEN-1 upstream inhibitor	TCTGTGCCTGGAATGATGTTCAACCAGCTAGGATTTGGTGTTTGTTGTTGGT
DEN-1 SCS	CAAACTCCTCTTAGGTCGAAAACTAAGAGAATGATGrAGTTTGGTGT
DEN-2 target	ACTGCTCTTAACATCCTC
DEN-2 upstream DNAzyme	ACATCCTC**TCCGAGCCGGTCGAA**CATCATTC
DEN-2 upstream inhibitor	TCTGTGCCTGGAATGATGTTCAACCAGCTAGGAGAGGATGTTAAGAGCAGT

DEN-2 SCS	CCTCCTCCTCTTAGGTCGAAAACTAAGAGAATGATGrAGGAGGATGT
DEN-3 target	GTGTGCCAGTCTTCAAGC
DEN-3 upstream DNAzyme	CTTCAAGC**TCCGAGCCGGTCGAA**CATCATTC
DEN-3 upstream inhibitor	TCTGTGCCTGGAATGATGTTCAACCAGCTAGGAGCTTGAAGACTGGCACAC
DEN-3 SCS	AAGCCTCCTCTTAGGTCGAAAACTAAGAGAATGATGrAGGCTTGAAG
DEN-4 target	TATTGAAGTCAGGCCACT
DEN-4 upstream DNAzyme	AGGCCACT**TCCGAGCCGGTCGAA**CATCATTC
DEN-4 upstream inhibitor	TCTGTGCCTGGAATGATGTTCAACCAGCTAGGAAGTGGCCTGACTTCAATA
DEN-4 SCS	CACTCTCCTCTTAGGTCGAAAACTAAGAGAATGATGrAGAGTGGCCT
DengueA target	CATCATTCCAGGCACAGA
DengueB target	CATGGGCTACTGGATAGA
Downstream DNAzyme	TGGATAGA**TCCGAGCCGGTCGAA**AACTAAGA
Downstream inhibitor	CATTCTCTTAGTTTTCGACCAGCTAGGATCTATCCAGTAGCCCATG
Downstream reporter substrate	/FAM/-TCTTAGTTrAGTCTATCCAAT-/TAM/

Table S3. Sequences from demonstration that SCS cleavage is necessary for signal propagation (Figure S2).

Strand	**Sequence**
Upstream DNAzyme	ATCACGCC**TCCGAGCCGGTCGAA**AGTATGTA
Uncleavable SCS	CGCCCTAATCTTAGGTCGAAAACTAAGATACATACTAGGGCGTGATG
SCS	CGCCCTAATCTTAGGTCGAAAACTAAGATACATACTrAGGGCGTGATG
Downstream DNAzyme	GAACTATC**TCCGAGCCGGTCGAA**AACTAAGA
Downstream inhibitor	ATGTATCTTAGTTTTCGACCGGC
Downstream reporter substrate	/FAM/-TCTTAGTTrAGGATAGTTCAT-/TAM/

Table S4. Sequences from demonstration of first SCS input-output combination (Figure S3a).

Strand	Sequence
Upstream DNAzyme	ATCACGCC**TCCGAGCCGGTCGAA**AGTATGTA
Upstream inhibitor	CTCCTGTGCATACATACTTTCAACCAGCTAGGAGGCGTGATGAT GAGTTTG
Input 1	AGTATGTATGCACAGGAG
Input 2	CAAACTCATCATCACGCC
SCS	CGCCCTAATCTTAGGTCGAAAACTAAGATACATACTrAGGGCGT GATG
Downstream DNAzyme	GAACTATC**TCCGAGCCGGTCGAA**AACTAAGA
Downstream inhibitor	ATGTATCTTAGTTTTCGACCGGC
Downstream reporter substrate	/FAM/-TCTTAGTTrAGGATAGTTCAT-/TAM/

Table S5. Sequences from demonstration of second SCS input-output combination (Figure S3b).

Strand	Sequence
Upstream DNAzyme	ATCACGCC**TCCGAGCCGGTCGAA**AGTATGTA
Upstream inhibitor	AAACATACATACTTTCGACCGGC
Input	GGTCGAAAGTATGTATGTTT
SCS	CGCCCTAATCTTAGGTCGAAAACTAAGATACATACTrAGGGCGT GATG
Downstream DNAzyme	TGATAGTTCATGTATCTTAGTTTTCGGAACTATC**AGCGATGACT GTTTTCAGTCCACCCATGT**AACTAAGA
Downstream reporter substrate	/FAM/-TCTTAGTTrAGGATAGTTCAT-/TAM/

Table S6. Sequences from demonstration of third SCS input-output combination (Figure S3c).

Strand	Sequence
Upstream DNAzyme	ATCACGCC**TCCGAGCCGGTCGAA**AGTATGTA
Upstream inhibitor	AAACATACATACTTTCGACCGGC
Input	GGTCGAAAGTATGTATGTTT
SCS	CGCCCTAATCTTAGGTCGAAAACTAAGATACATACTrAGGGCGT GATG
Downstream	/FAM/-GCCGGTCGAAAACTAAGA

fluorophore strand	
Downstream quencher strand	ATGTATCTTAGTTTTCGACC-/TAM/

Table S7. Sequences from optimization of DEN-3 serotyping circuit (Figure S5b).

Strand	Sequence
Initial DEN-3 target	TGCCAGTCTTCAAGCATG
Initial DEN-3 upstream DNAzyme	CAAGCATG**TCCGAGCCGGTCGAA**CATCATTC
Initial DEN-3 upstream inhibitor	TCTGTGCCTGGAATGATGTTCAACCAGCTAGGACATGCTTGAAGACTGGCA
Initial DEN-3 SCS	CATGCTCCTCTTAGGTCGAAAACTAAGAGAATGATGrAGCATGCTTG
Optimized DEN-3 target	GTGTGCCAGTCTTCAAGC
Optimized DEN-3 upstream DNAzyme	CTTCAAGC**TCCGAGCCGGTCGAA**CATCATTC
Optimized DEN-3 upstream inhibitor	TCTGTGCCTGGAATGATGTTCAACCAGCTAGGAGCTTGAAGACTGGCACAC
Optimized DEN-3 SCS	AAGCCTCCTCTTAGGTCGAAAACTAAGAGAATGATGrAGGCTTGAAG
DengueA target	CATCATTCCAGGCACAGA
DengueB target	CATGGGCTACTGGATAGA
Downstream DNAzyme	TGGATAGA**TCCGAGCCGGTCGAA**AACTAAGA
Downstream inhibitor	CATTCTCTTAGTTTTCGACCAGCTAGGATCTATCCAGTAGCCCATG
Downstream reporter substrate	/FAM/-TCTTAGTTrAGTCTATCCAAT-/TAM/

Table S8. Sequences from optimization of DEN-2 serotyping circuit (Figure S5d).

Strand	Sequence
Initial DEN-2 target	CTCTTAACATCCTCACAG
Initial DEN-2 upstream DNAzyme	CCTCACAG**TCCGAGCCGGTCGAA**CATCATTC
Initial DEN-2 upstream inhibitor	TCTGTGCCTGGAATGATGTTCAACCAGCTAGGACTGTGAGGATGTTAAGAG

Initial DEN-2 SCS	ACAGCTCCTCTTAGGTCGAAAACTAAGAGAATGATGrAGCTGTGAGG
Optimized DEN-2 target	ACTGCTCTTAACATCCTC
Optimized DEN-2 upstream DNAzyme	ACATCCTC**TCCGAGCCGGTCGAA**CATCATTC
Optimized DEN-2 upstream inhibitor	TCTGTGCCTGGAATGATGTTCAACCAGCTAGGAGAGGATGTTAAGAGCAGT
Optimized DEN-2 SCS	CCTCCTCCTCTTAGGTCGAAAACTAAGAGAATGATGrAGGAGGATGT
DengueA target	CATCATTCCAGGCACAGA
DengueB target	CATGGGCTACTGGATAGA
Downstream DNAzyme	TGGATAGA**TCCGAGCCGGTCGAA**AACTAAGA
Downstream inhibitor	CATTCTCTTAGTTTTCGACCAGCTAGGATCTATCCAGTAGCCCATG
Downstream reporter substrate	/FAM/-TCTTAGTTrAGTCTATCCAAT-/TAM/

SUPPLEMENTARY DISCUSSION 1

Discussion of spurious interactions in cascades

We have identified the following potential mechanisms for spurious activation in our DNAzyme signaling cascades.

1. Unwanted activation of one of the DNAzymes in the cascade by spontaneous dissociation of its inhibitor. The spuriously activated DNAzyme can then proceed to cleave its substrate, which may be an SCS molecule or a fluorescently labeled readout substrate.
2. Unwanted binding of an inhibited upstream DNAzyme to the SCS molecule. This may open the outer stem even in the absence of a cleavage reaction, providing a window of opportunity for the downstream effector sequence to interact with the downstream, inhibited DNAzyme.
3. Direct binding of the downstream inhibitor toehold to the sequestered toehold in the outer loop, leading to activation of the downstream DNAzyme by a toehold-mediated strand displacement (TMSD) reaction.
4. Spontaneous dissociation of one or both of the duplex stems of the SCS molecule, which reduces the topological constraint on the downstream toehold, enabling it to more easily activate the downstream DNAzyme by TMSD.

Our design work on DNAzyme displacement logic gates has shown that the effect of mechanism #1 can be reduced by extending the length of the inhibitor strands and, if necessary, introducing additional inhibitor strands free in solution to bias the equilibrium towards continued deactivation of the DNAzymes.

We addressed mechanism #2 by running additional controls with an SCS molecule in which the RNA base at the cleavage site is replaced by the corresponding DNA base. Since the 8-17 DNAzyme is RNA-cleaving, this single base substitution suffices to make the SCS molecule uncleavable by the upstream DNAzyme (Figure S3). These results demonstrated that stem opening by the binding of the upstream DNAzyme is not a significant leak mechanism.

Previous studies of hairpin opening kinetics [17] have shown that the rate constant for opening a hairpin by TMSD is several orders of magnitude slower when the toehold is contained within the hairpin (an “internal toehold”) as opposed to outside (an “external toehold”). This is directly relevant to the kinetics of unwanted binding of the downstream, inhibited DNAzyme to the sequestered our SCS molecule, as in mechanism #3, which can be thought of as opening a loop via an internal toehold. Hence we conclude that mechanism #3 is probably not the dominant leakage mechanism.

Therefore, mechanism #4 is most likely to be the primary source of leakage in our cascades. The most obvious way to reduce such spurious dissociation of duplexes in the SCS molecule would be to extend these duplexes, in order to increase their melting temperature. However, the desire to retain multiple turnover in the cleavage of SCS molecules by upstream DNAzymes restricts the length of the DNAzymes’ substrate binding arms to ~8-10 nucleotides each, so that the product strands unbind rapidly from the DNAzyme after cleavage. This, in turn, places upper limits on the lengths of the duplexes in the SCS structure, since these must be displaced by the substrate binding arms via TMSD reactions. One of the substrate binding arms must also bind to the SCS toehold, so this also had to be taken into consideration when designing the basic SCS

structure. A 4nt toehold was chosen to strike a balance between speed of toehold binding and subsequent strand displacement, and leaving enough of the substrate binding arm left so that the stem could be sufficiently long to reduce leakage as far as possible.

Discussion of rate-limiting steps in DNAzyme signaling cascades

Cleavage of an SCS molecule by an active upstream DNAzyme is a complex reaction with a number of steps that could be rate-limiting. In particular:

1. In order to cleave the SCS molecule, the upstream DNAzyme must initiate a TMSD reaction to open the outer stem and then nucleate a second binding event with the outer loop, so that both substrate binding arms are bound to the SCS molecule and the catalytic core is correctly positioned opposite the cleavage site. The second binding event is similar to a "remote toehold" strand displacement reaction [18], in that an internal diffusion step is required, which slows down the reaction considerably. Furthermore, the cleavage reaction must compete with the attempts of the SCS molecule to reform its dual-stem structure. This could cause the upstream DNAzyme to be displaced from the complex before cleavage takes place.
2. Post-cleavage, activation of the downstream DNAzyme involves a TMSD reaction in which the invading strand has some secondary structure (the short hairpin comprising the inner stem and inner loop from Figure 1a), as opposed to being a single strand with no secondary structure. It is well known that secondary structure in the invader strand reduces the rate of strand displacement reactions [19].

Discussion of SCS design parameters and circuit leakage

The design of the SCS balances a number of constraints. To minimize the rate of leakage, that is, unwanted downstream activation caused by uncleaved SCS molecules interacting with DNAzyme gates, stems were made as long as possible. However, for efficient catalytic turnover the substrate binding arms of the DNAzymes should each be at most 8 nucleotides long, constraining the length of the stems [20]. To maximize the length of the outer stem and toehold while respecting this constraint, we place the cleavage site within the outer stem. Finally, to reduce leakage we make the SCS as compact as possible, by using the outer loop (part of the input module) to also serve as the toehold for the downstream activator. Minimizing loop size makes them more difficult to invade when in the sequestered state, reducing the potential for unwanted circuit element interactions. This approach does not constrain the recognition sequences of the different DNAzymes in the cascade. Overall, our SCS design exploits the predictable, sequence-specific folding of DNA to program a favorable reaction pathway directly into the structure of the substrate molecule.

Despite these efforts, the primary limiting factor for DNAzyme signaling cascades using the SCS remains the rate of circuit leakage. Although constraints on the SCS limit design space to a certain extent, a number of alternative strategies offer the potential to overcome this challenge. These include the physical separation of circuit components by attaching them to the surfaces of microspheres [21, 22], and the rational introduction of mismatched bases [23] in the SCS design. Such strategies may be used in conjunction with one another, as physical separation should reduce the number of interactions between inactivate circuit components, while mismatches should reduce the conditional probability of unwanted signal generation given that an interaction has taken place. A number of such design alternatives are currently being explored. Additionally, while our

work has advanced DNA logic for bioassay development, several challenges still remain. Most notable is the use of the fluorogenic chimeric substrate, which is expensive and requires RNAse free conditions for optimal response. However, recent work on DNA cleaving DNAzymes [14-16] may offer a path forward using cheaper pure DNA substrates instead of chimeric DNA/RNA substrates.

REFERENCES

1. Breaker, R.R. and G.F. Joyce, *A DNA enzyme with Mg(2+)-dependent RNA phosphoesterase activity.* Chem Biol, 1995. **2**(10): p. 655-60.
2. Santoro, S.W. and G.F. Joyce, *A general purpose RNA-cleaving DNA enzyme.* Proc Natl Acad Sci U S A, 1997. **94**(9): p. 4262-6.
3. Dirks, R.M., et al., *Thermodynamic analysis of interacting nucleic acid strands.* SIAM Rev, 2007. **49**(1): p. 65-88.
4. Fanning, M.L., J. Macdonald, and D. Stefanovic, *ISO: numeric representation of nucleic acid form*, in *ACM-BCB 2011*. 2011, ACM.
5. Zadeh, J.N., B.R. Wolfe, and N.A. Pierce, *Nucleic acid sequence design via efficient ensemble defect optimization.* J Comput Chem, 2011. **32**(3): p. 439-52.
6. SantaLucia, J., Jr., *A unified view of polymer, dumbbell, and oligonucleotide DNA nearest-neighbor thermodynamics.* Proc Natl Acad Sci U S A, 1998. **95**(4): p. 1460-5.
7. Kim, H.-K., et al., *Dissecting metal ion–dependent folding and catalysis of a single DNAzyme.* Nat Chem Biol, 2007. **3**(12): p. 763-768.
8. Mazumdar, D., et al., *Activity, folding and Z-DNA formation of the 8-17 DNAzyme in the presence of monovalent ions.* J Am Chem Soc, 2009. **131**(15): p. 5506-5515.
9. Kim, H.K., et al., *Probing metal binding in the 8–17 DNAzyme by TbIII luminescence spectroscopy.* Chem Eur J, 2008. **14**(28): p. 8696-8703.
10. Okumoto, Y. and N. Sugimoto, *Effects of metal ions and catalytic loop sequences on the complex formation of a deoxyribozyme and its RNA substrate.* J Inorg Biochem, 2000. **82**(1-4): p. 189-95.
11. Faulhammer, D. and M. Famulok, *Characterization and divalent metal-ion dependence of in vitro selected deoxyribozymes which cleave DNA/RNA chimeric oligonucleotides.* J Mol Biol, 1997. **269**(2): p. 188-202.
12. Brown, C.W., III, et al., *Catalytic molecular logic devices using DNAzyme displacement.* ChemBioChem, 2014. **15**: p. 950-954.
13. Zhang, D.Y., *Cooperative hybridization of oligonucleotides.* J Am Chem Soc, 2011. **133**(4): p. 1077-86.
14. Chandra, M., A. Sachdeva, and S.K. Silverman, *DNA-catalyzed sequence-specific hydrolysis of DNA.* Nat Chem Biol, 2009. **5**(10): p. 718-720.
15. Gu, H., et al., *Small, Highly Active DNAs That Hydrolyze DNA.* J Am Chem Soc, 2013. **135**(24): p. 9121-9129.
16. Xiao, Y., et al., *Establishing broad generality of DNA catalysts for site-specific hydrolysis of single-stranded DNA.* Nucleic Acids Res, 2012. **40**(4): p. 1778-1786.
17. Green, S.J., D. Lubrich, and A.J. Turberfield, *DNA hairpins: fuel for autonomous DNA devices.* Biophys J, 2006. **91**(8): p. 2966-75.
18. Genot, A.J., et al., *Remote toehold: a mechanism for flexible control of DNA hybridization kinetics.* J Am Chem Soc, 2011. **133**(7): p. 2177-82.
19. Gao, Y., L.K. Wolf, and R.M. Georgiadis, *Secondary structure effects on DNA hybridization kinetics: a solution versus surface comparison.* Nucleic Acids Res, 2006. **34**(11): p. 3370-7.
20. Santoro, S.W. and G.F. Joyce, *Mechanism and utility of an RNA-cleaving DNA enzyme.* Biochemistry, 1998. **37**(38): p. 13330-42.
21. Frezza, B.M., S.L. Cockroft, and M.R. Ghadiri, *Modular multi-level circuits from immobilized DNA-based logic gates.* J Am Chem Soc, 2007. **129**(48): p. 14875-14879.

22. Yashin, R., S. Rudchenko, and M.N. Stojanovic, *Networking particles over distance using oligonucleotide-based devices.* J Am Chem Soc, 2007. **129**(50): p. 15581-4.
23. Jiang, Y.S., et al., *Mismatches Improve the Performance of Strand-Displacement Nucleic Acid Circuits.* Angew Chem Int Ed, 2014. **53**(7): p. 1845-1848.